PDMS Melts on Mica Studied by Confocal Raman Scattering†

Shan Jiang, Sung Chul Bae, and Steve Granick*

Departments of Materials Science and Engineering, Chemistry, and Physics, University of Illinois, Urbana, Illinois 61801

Received July 28, 2007. In Final Form: September 8, 2007

We report surprising surface-induced torsional alignment of polydimethylsiloxane (PDMS) chains in contact with the muscovite (001) mica surface with and without confinement. The alignment was measured by polarized confocal Raman spectroscopy over diffraction-limit circular spots with ∼0.3 μm diameter. Our discussion here focuses on the intense symmetric methyl-group vibration centered at 2907 cm^{-1}, whose Raman scattering intensity is found to depend on whether incident light is polarized in the *x* or *y* direction of the surface, the *x* direction being parallel to one of the mica optical axes. Furthermore, the Raman peak broadens significantly relative to that of bulk PDMS while remaining Lorentzian in shape, implying slower but homogeneous vibrational dephasing. However, the preferred orientation differs, apparently stochastically, from spot to spot on the surface. Possible origins of this heterogeneous surface-induced structure are discussed.

Introduction

Structure, organization, and dynamics of confined molecules underly much of the lubrication function. In spite of the rich information that comes from theory and computer simulation[1,2] regarding the arrangement and packing of confined molecules, there exists too little direct experimental information on this fundamental point. The main experiments are predicated on observations using force microscopy, primarily the surface forces apparatus (SFA) and atomic force microscopy (AFM), which have evolved the capability to measure mechanical forces under ever better defined experimental conditions. However, a great limitation of the experiments performed in this spirit is that, while informative about mechanical response, the information is not chemical. Thus, while it is known that normal and friction forces oscillate with the periodicity of the molecular dimension, showing that fluids tend to form ordered layers in the direction normal to surfaces[3] (which is expected by analogy to the radial distribution function of molecules in bulk fluids), information at a chemical level is also desirable.

Optics-based experiments can, in principle, overcome this limitation. Though the power of spectroscopic techniques in the study of confined fluid has been of speculative interest to many researchers for a long time, few successes have been reported. Within the surface forces apparatus, Safinya and co-workers investigated the structure of a thin smectic liquid crystal film under micrometer-level confinement using synchrotron X-ray scattering,[4] but the technique was not used to study ultrathin (∼1 nm thick) liquid films. Synchrotron waveguide methods were used to characterize the layering of molecularly thin films.[5] The microrheometer developed by Dhinojwala and co-workers can be combined with infrared spectroscopy, dielectric spectroscopy, and scattering (X-ray and neutron) techniques,[6] and so also can a microrheometer developed by McKinley and co-workers,[7] but both these methods are best suited for thicker (0.1 μm to 10 μm) films. By utilizing a prism as one of the opposed surfaces, recently rheometry was combined with nonlinear spectroscopy, specifically the surface-sensitive technique of infrared−visible sum frequency generation (SFG) in the total internal reflection geometry.[8−10] That combination can be used to probe the orientation, alignment, and relaxation modes of organic molecules at a buried interface in a condition of flow or shear. Some years back, it was also shown that SFG can be combined with the surface forces apparatus (SFA) to study nanometer-thick films of a self-assembled monolayer confined between atomically smooth mica surfaces,[11] but implementation of this approach to other experimental situations has not been reported as yet. In addition, this laboratory has used fluorescence correlation spectroscopy (FCS) to measure how diffusion is modified when molecules are confined into molecule-thin films.[12−14]

Here, we describe findings using confocal Raman scattering. The novel point is to employ *unenhanced* Raman scattering, which more typically is restricted to studying bulk fluids or fluids in pores[15,16]—this is so because of the intrinsic low sensitivity of this method. The reason we have not employed surface-enhanced Raman spectroscopy (SERS) is that this method to enhance sensitivity depends on having a metal surface with high local curvature—it is incompatible with measuring effects between atomically smooth solids. The evident difficulty, in using unenhanced Raman scattering, is that to obtain needed signal-

† Part of the Molecular and Surface Forces special issue.

(1) Bhushan, B.; Gupta, B. K. *Handbook of Tribology: Materials, Coatings, and Surface Treatments*; Krieger Publishing Company, 1997.
(2) Bhushan, B.; Israelachvili, J. N.; Landman, U. *Nature* **1995**, *374*, 607−616.
(3) Israelachvili, J. N. *Intermolecular and Surface Forces*; Academic Press: London, 1992.
(4) Golan, Y.; Seitz, M.; Luo, C.; Martin-Herranz, A.; Yasa, M.; Li, Y. L.; Safinya, C. R.; Israelachvili, J. *Rev. Sci. Instrum.* **2002**, *73*, 2486−2488.
(5) Seeck, O. H.; Kim, H.; Lee, D. R.; Shu, D.; Kaendler, I. D.; Basu, J. K.; Sinha, S. K. *Europhys. Lett.* **2002**, *60*, 376−382.
(6) Soga, I.; Dhinojwala, A.; Granick, S. *Langmuir* **1998**, *14*, 1156−1161.
(7) McKinley, G. Private communication.
(8) Fraenkel, R.; Butterworth, G. E.; Bain, C. D. *J. Am. Chem. Soc.* **1998**, *120*, 203−204.
(9) Du, Q.; Xiao, X. D.; Charych, D.; Wolf, F.; Frantz, P.; Shen, Y. R.; Salmeron, M. *Phys. Rev. B* **1995**, *51*, 7456−7463.
(10) Mamedov, S.; Schwab, A. D.; Dhinojwala, A. *Rev. Sci. Instrum.* **2002**, *73*, 2321−2324.
(11) Frantz, P.; Wolf, F.; Xiao, X. D.; Chen, Y.; Bosch, S.; Salmeron, M. *Rev. Sci. Instrum.* **1997**, *68*, 2499−2504.
(12) Mukhopadhyay, A.; Zhao, J.; Bae, S. C.; Granick, S. *Rev. Sci. Instrum.* **2003**, *74*, 3067−3072.
(13) Mukhopadhyay, A.; Bae, S. C.; Zhao, J.; Granick, S. *Phys. Rev. Lett.* **2004**, *93*, 236105.
(14) Mukhopadhyay, A.; Zhao, J.; Bae, S. C.; Granick, S. *Phys. Rev. Lett.* **2002**, *89*, 136103.
(15) Zhu, X.; Farrer, R. A.; Fourkas, J. T. *J. Phys. Chem. B* **2005**, *109*, 12724−12730.
(16) Yi, J.; Jonas, J. *J. Phys. Chem.* **1996**, *100*, 16789−16793.

10.1021/la702295y CCC: $40.75
Published on Web 11/15/2007

to-noise from nanometer-thick films requires the utmost optimization of the optical setup.[17,18]

The choice of experimental system in this paper was decided with the following considerations in mind. First, the molecule must possess unusually intense Raman-active vibrations. For example, the carbon−carbon bond of alkanes is inappropriate owing to its low Raman scattering cross section. After screening a large number of fluids, we have found the methyl (CH_3) on polydimethylsiloxane (PDMS) and the cyano (C≡N) group vibrations on various other molecules to be especially suited to the purpose. The present study focuses on the former, while a paper in preparation focuses on the cyano group in 6CB, a nematic liquid crystal. Second, these Raman-active vibrations should be indicative of how the fluid orients in the $x-y$ plane of the solid that confines them between parallel plates. That is why the methyl vibrations on a compact-shaped molecule, for example, of octamethylcyclotetrasiloxane (OMCTS, which has been widely studied by force microscopy[13]), are inappropriate because their placement on the molecule is symmetric. Third, the fluid should be stable chemically (lacking C═C bonds, for example), capable of sustaining the high laser intensity necessary to measure Raman scattering from nanometer-thick films.

These are the reasons we selected for study the polymer liquid, PDMS. From force microscopy and X-ray reflectivity, the expected layering of this fluid is known. Periodicity in the force−distance profile is known from SFA experiments.[19] This was extended at length recently using AFM.[20] That shear can enhance the layering of PDMS has been inferred from measurements of friction when it is sheared between mica surfaces.[21] Although computer simulations suggest that surface roughness lessens long-range layering and can cause it even to disappear,[22−24] sum-frequency generation shows[25,26] that, with some rough solid surfaces, polymer chains will adopt a rather ordered structure under confinement, in the direction normal to the substrate, and this disappears when confinement is released. Synchrotron X-ray reflectivity measurements of a low molecular weight PDMS layer on a single silicon surface also give evidence of layered structure.[27] All these studies focused on the layered or ordered structure of the polymer in the direction normal to the surface.

Here, we explore the different question of molecular conformation in the plane of the confining surfaces. A confocal geometry is employed in order to obtain microscopic spectra from different areas of the confined film, thus measuring possible heterogeneities from spot to spot. A preliminary account of these experiments has been published elsewhere.[17]

Experimental Section

To enable these experiments, the surface forces apparatus was redesigned while still maintaining use of muscovite mica as the confining surface.

The traditional method to determine surface−surface separation and contact area, in a surface forces apparatus, employs a silver layer placed at the backside of mica for this purpose. A severe limitation is that the high reflectivity of silver from the infrared to UV regime excludes optical experiments of the kind that we describe below. To remedy this, silver coatings on the backside of mica were replaced by multilayer dielectric coatings deposited using electron beam deposition. In our original publication on this subject, thirteen layers of TiO_x and Al_2O_3 were grown by electron-beam evaporation,[14] and the optical thickness of each layer was approximately $\lambda/4$ ($\lambda \sim$ 650 nm) as determined by the optical monitor within the coating chamber. The desired thickness of each coating was calculated using software (J. A. Woolam Co., Inc., Lincoln, NE) so that the spectral windows of reflectivity and translucency were controlled by the deposition conditions. However, the use of TiO_x is found to enhance background fluorescence, lowering signal to noise in the Raman measurements. This laboratory's most recent experiments employ HfO_x instead, and only nine alternate layers are found to suffice. Using these dielectric coatings, one obtains one region in the optical spectrum of high reflectivity where the surface−surface separation can be measured by traditional multiple-beam interferometry of incident white light and a second region of high transmission needed for Raman spectroscopy studies.

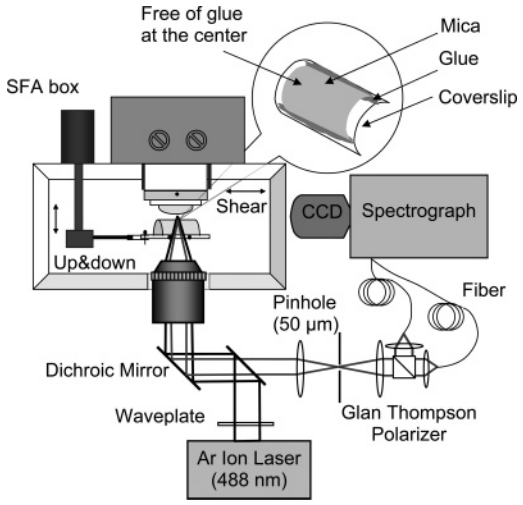

Figure 1. Schematic diagram of the modified surface forces apparatus adapted for confocal Raman spectroscopy. Key elements of this home-built setup include (a) long working distance objective through which incident light is focused to the sample and scattered Raman signal is collected; (b) dielectric coatings on the back side of mica surfaces that are transparent to this light, yet reflective at higher wavelength, enabling film thickness to be determined by multiple beam interferometry; (c) bottom mica surface that sits closer to the microscope objective than typically possible in a surface forces apparatus. The symbols x and y in the text refer to the two orthogonal directions in plane of the mica surface, with x parallel to the shear direction as shown in this plot. Other details of the experimental setup are described in the text.

In the experiments described below, Raman scattering was produced by the 488 nm of an Ar^+ laser (Melles-Griot, 543-BS-AO3), and the dielectric coatings were grown to be highly transparent in the region 430 to 590 nm. To protect the dielectric coating exposed under the tightly focused laser beam of high power, a 1 nm layer of aluminum oxide was deposited to cover the outer surface.

Figure 1 shows a schematic diagram of the home-built optical setup. The polarization of the incoming laser beam was controlled using a half-wave plate. The laser beam overfilled an objective lens to obtain a diffraction-limited beam size and was presented to the sample through an objective described below. The scattered Raman signal was collected by the same objective lens and was focused to a pinhole by a tube lens in order to reject out-of-focus signals including fluorescence background from mica sheets and supporting lenses. After filtering laser scattering using a holographic notch filter, the scattered Raman signal was dispersed using a SpectraPro 2300i spectrometer (Acton) and was detected using a liquid-nitrogen-cooled CCD (Roper Scientific LN/CCD-1340/400-EB/1). The pinhole

(17) Bae, S. C.; Lee, H.; Lin, Z. Q.; Granick, S. *Langmuir* **2005**, *21*, 5685−5688.
(18) Beattie, D. A.; Winget, S. A.; Bain, C. D. *Tribol. Lett.* **2007**, *27*, 1573−2711.
(19) Horn, R. G.; Israelachvili, J. N. *Macromolecules* **1988**, *21*, 2836−2841.
(20) Sun, G. X.; Kappl, M.; Butt, H. J. *Eur. Polym. J.* **2005**, *41*, 663−667.
(21) Yamada, S. *Langmuir* **2003**, *19*, 7399−7405.
(22) Frink, L. J. D.; van Swol, F. *J. Chem. Phys.* **1998**, *108*, 5588−5598.
(23) Gao, J. P.; Luedtke, W. D.; Landman, U. *Tribol. Lett.* **2000**, *9*, 3−13.
(24) Ghatak, C.; Ayappa, K. G. *J. Chem. Phys.* **2004**, *120*, 9703−9714.
(25) Nanjundiah, K.; Dhinojwala, A. *Phys. Rev. Lett.* **2005**, *95*, 154301.
(26) Yurdumakan, B.; Harp, G. P.; Tsige, M.; Dhinojwala, A. *Langmuir* **2005**, *21*, 10316−10319.
(27) Evmenenko, G.; Dugan, S. W.; Kmetko, J.; Dutta, P. *Langmuir* **2001**, *17*, 4021−4024.

diameter was 50 μm. At the spectrometer, a narrow (100 μm) entrance slit was used to minimize instrumental broadening and thus enable bandwidth analysis, as described in the Results section.

The experiments presented below employ an objective with an exceptionally long working distance of 1.57 mm (Zeiss LD Achroplan 63× Ph2, NA = 0.75). In addition to possessing a long working distance, an advantage of this lens is a correction collar on the objective, used to compensate aberration as light traverses glass on which the mica sheets are mounted. The correction collar was found to boost signal intensity by ∼2−3 times. This is a change from our preliminary experiments[17] that employed, as the objective, an aspheric lens. An aspheric lens is considerably less expensive (a factor of at least 10) and combines a reasonably high numerical aperture (NA = 0.68) with a long working distance. However, the efficiency was found to be less than for more elaborate objectives, and the aspheric lens was found to introduce severe chromatic aberration, making it difficult to optimize the pinhole position.

When measuring the vibrational line shape, the polarized and depolarized Raman signals were measured simultaneously, separated by a Glan-Tayler analyzer, and the separated signals were delivered to the spectrometer by separate optical fibers. The two channels were calibrated before each experiment using bulk PDMS melt.

Modifications were also made to the traditional method of mounting mica for surface forces studies. To minimize the distance between the microscope objective and the sample, a cylindrical support for the bottom mica sheet was formed before each experiment simply by heating a Pyrex microscope cover glass in a Bunsen burner, letting gravity bend it to the desired radius of curvature. To minimize background fluorescence and Raman scattering from the adhesive used to attach mica sheets to a cylindrical lens in these experiments, adhesive was applied only at the boundary of the mica sheet, not at the center where Raman measurements were made. This resulted in a flattened contact area at the apex of the crossed cylinders over which the mica was draped, the application of normal pressure causing the cylindrical mica sheets to deform. For added mechanical stiffness, thick mica sheets (∼5−10 μm) were used.

In interferometry measurements of surface separation to determine thickness of the liquid film, the interferometric fringes were fitted to a Lorentzian line shape as described elsewhere,[28] giving a resolution of ±4 Å in spite of having unusually thick mica sheets.

The Raman bands were fit using *Peakfit* (AISN Software Inc.), and this program was also used to subtract the background. All the analyses within a single experiment were carried out using the same set of fitting parameters, and error bars were calculated on the basis of the fitting error. In measuring anisotropy using polarized radiation, the setup was calibrated by using the bulk PDMS sample before each measurement and consecutive measurements were made to ensure that the change in the intensity did not come from instability of the setup. Signals were averaged for ∼15 min. The anisotropy was calculated only when the signal intensity could be recovered by two consecutive measurements under the same laser polarization.

Freshly cleaved mica sheets were prepared using the method of Israelachvili[29] and Klein,[30] which has the advantage that it is straightforward to prepare the thick sheets of mica needed for these experiments. The mica sheets were oriented to be parallel to one another. In some experiments, shear displacements were applied, shear being parallel to the optical axis of the mica, as will be described elsewhere. A preliminary account of the effects of shear has been presented.[17]

The PDMS (molecular-average molecular weight M_w = 7060 g-mol^{-1}, polydispersity = 1.07) was purchased from Polymer Source and used as received. In some control experiments regarding polymer orientation at a *single* mica surface, the freshly cleaved mica sheet was dipped into dilute PDMS (M_w= 2400 g/mol, polydispersity = 1.18, Polymer Source) solutions of 2−20 mg/mL and was withdrawn at a constant speed of 1 mm/s. Finally, the sample was dried at room temperature for at least 1 day.

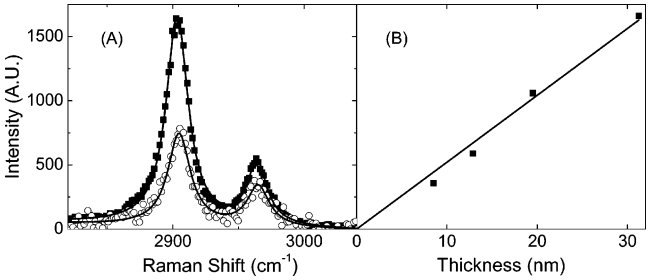

Figure 2. Illustrations of raw data for Raman scattering. Panel A shows intensity plotted against wavelength in the methyl-stretch region, showing the symmetric stretch centered at 2907 cm^{-1} and the asymmetric stretch centered at 2965 cm^{-1}. Squares: data for bulk PDMS melt; data acquired in 1 s. Circles: data for a thin film 10 nm thick; data acquired in 10 min. The lines are fits to the expected Lorentzian function after subtracting the background. Panel B. For PDMS confined between two opposed mica sheets, peak intensity of the symmetric stretch at 2907 cm^{-1} is plotted against film thickness *d*.

Results and Discussion

While the siloxane (Si−O) vibration along the backbone of the PDMS chain affords in principle the most direct measure of in-plane orientation, its intensity is too weak to be detected in the thinnest films; this we showed in detail in an earlier paper.[17] However, the more intense stretching vibrations of the methyl group are nearly perpendicular to the polymer backbone; this too is illustrated in an earlier paper.[17] When illuminated by polarized light, anisotropy in the $x-y$ plane of the methyl-group Raman bands indicates that, averaged over the confocal spot, methyl groups orient preferentially in a distinct direction parallel to the confining surfaces. Since we are measuring the vibration of the methyl group, the net orientation of this small side group does not necessarily indicate the orientation of the whole backbone of the PDMS chains but instead indicates a net torsional orientation.

Measurements can be made at different confocal spots, each of them with ∼0.3 μm, providing a spatial image of Raman scattering at different positions—not just within the flattened center of the Hertzian contact, but also progressively farther away as the crossed cylinders curve away from one another. Simultaneously, the local thickness of the PDMS film at each spot can be measured using multiple beam interferometry.

In Figure 2B, peak Raman scattering intensity of the symmetric methyl group is plotted against local film thickness, and one observes the linear relation expected from Beer's law. Note that the constant of proportionality can differ by a factor of up to 2 in repeated independent measurements of this kind, as it is not practical to focus the confocal spot (∼1 μm high) perfectly centered within a thin film a few nanometers thick. Independent measurements of this kind do invariably show linearity, however, and this we consider to be the main point.

Figure 2A illustrates the nature of raw data in more detail. Raman scattering intensity is plotted against wavenumber in the methyl stretch region; one observes not only the symmetric peak analyzed in this paper (centered at 2907 cm^{-1}), but also the less intense asymmetric peak (centered at 2965 cm^{-1}), approximately 3 times weaker. The ratio between the symmetric and asymmetric peak intensity was analyzed and discussed by this laboratory earlier.[17] In the graphs presented below, we analyze especially

(28) Wong, J. S.; Bae, S. C.; Anthony, S.; Zhu, Y. X.; Granick, S. *Phys. Rev. Lett.* **2006**, *96*, 099602.
(29) Israelachvili, J. N.; Alcantar, N. A.; Maeda, N.; Mates, T. E.; Ruths, M. *Langmuir* **2004**, *20*, 3616−3622.
(30) Perkin, S.; Chai, L.; Kampf, N.; Raviv, U.; Briscoe, W.; Dunlop, I.; Titmuss, S.; Seo, M.; Kumacheva, E.; Klein, J. *Langmuir* **2006**, *22*, 6142−6152.

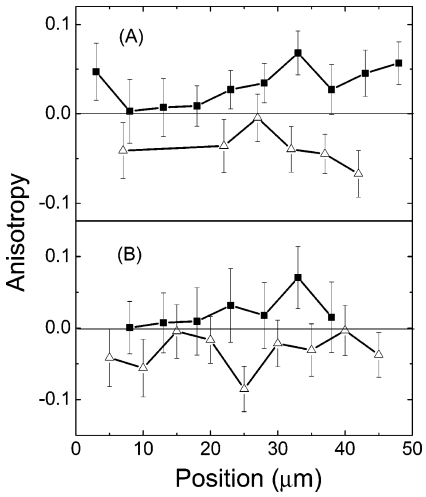

Figure 3. Local anisotropy of the symmetric methyl stretch in the $x-y$ plane, defined by eq 2, plotted against local spatial position for thin films of PDMS melt adsorbed on a single mica surface. Panels A and B refer to two independent experiments. Squares and triangles refer to measurements made before and after rotating the mica by 90°.

the more intense vibration, as parallel partial analysis of the less intense one showed that it follows the same pattern but with poorer signal to noise. A second point to notice in Figure 2B is the comparison of the signal intensity for the case of Raman scattering from bulk PDMS melt and from a thin film. For the bulk melt, 1 s sufficed to acquire a well-resolved spectrum with minimal noise in the data. For the film 10 nm thick, the data remain somewhat noisier even signal averaging for 10 min, which is a period 600 times longer, under the same laser power. In Figure 2A, lines through the data are fits to the expected Lorentzian line shape, and one observes that the fit is excellent.

Chains Possess Distinct Lateral Orientations that Differ from Spot to Spot. The pseudo-hexagonal lattice of cleaved muscovite mica is known to orient nematic liquid crystals in a preferred orientation,[31] so by Occam's razor we considered the possibility that the confinement-associated orientation reported below might exist similarly for thin PDMS melts on mica. These thin films were deposited by adsorption as described in the Experimental Section.

Measurements were made at different spots along the surface. The laser beam was polarized either parallel to or perpendicular to the mica optical axis, and the Raman anisotropy (A) was defined as the difference between the Raman scattering intensity excited by incident light with orthogonal polarization

$$A = \frac{I_x - I_y}{I_x + I_y} \tag{1}$$

where I_x and I_y represent the peak intensities of the symmetric methyl stretch vibration parallel to and perpendicular to the optical axis, respectively. This quantifies the planar anisotropy of the projection of PDMS chains onto the mica sheet.

Figure 3 summarizes two independent experiments in which, for a PDMS film ~2 nm thick (estimated from the Raman scattering intensity), a line scan of roughly 10 repeated measurements were made at different spatial positions. It is worthwile to mention that mica was always oriented with its optical axis aligned to the laser polarization, though we cannot identify whether it is short-axis or long-axis. The numbers for anisotropy are small, but it is striking that the anisotropy was

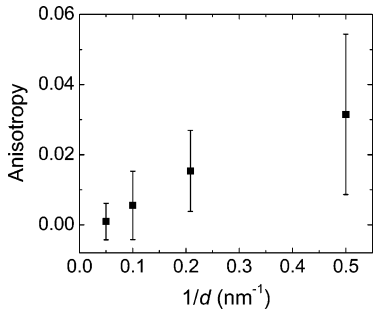

Figure 4. Mean anisotropy of the symmetric methyl stretch in the $x-y$ plane (defined by eq 2), averaged at many spatial positions, plotted against PDMS thickness for thin films of PDMS adsorbed on a single mica surface. The error bar is the standard deviation from more than 10 measurements.

finite at many (not all) of these spots; this indicates the existence of net lateral orientation over the diameter of the confocal spot. At some confocal locations, the net anisotropy falls to zero. Between confocal locations, the anisotropy varies stochastically.

It is not possible to quantify the amount of lateral ordering based on only two polarization measurements of the vibrations of methyl side groups; to do so requires measuring a wider range of azimuthal angles;[32] in addition, we want to emphasize that the orientation of the methyl symmetric stretch may not represent the orientation of the polymer backbone. However, it is remarkable that independent experiments are consistent in showing this variability. Figure 3 shows that the sign of local anisotropy changed when the mica sheet was rotated by 90°. This confirmed the validity of these measurements, although there is some quantitative variability, as it was not possible to make the repeat measurements at exactly the same positions as previously.

By exploring the dependence on thickness (d) of the polymer melt, Figure 4 shows that A increases as d gets smaller. The data are consistent with a linear dependence between A and $1/d$, which is the relation often observed for experiments in porous media and traditionally explained by a quasi "two-state model" consisting of parallel contributions from a surface layer and a separate bulk layer. The error bars are, however, too large to decide that the dependence is linear rather than weakly nonlinear. Furthermore, it is clear that, while a two-state model may describe the ensemble-average anisotropy, the actual anisotropy from point to point along the sample is more complex than can be fully described by so simple a model.

Similarly heterogeneous alignment was found when PDMS chains were confined between two opposed mica sheets inside a surface forces apparatus. Figure 5 shows line scans across the diameter of the Hertzian contact zones for three independent experiments; on the left ordinate axis, anisotropy is plotted, and on the right ordinate axis, the local film thickness is plotted. As for PDMS on a single mica surface, the net methyl alignment within the diameter of the confocal spot fluctuates from spot to spot, emphasizing some kind of heterogeneity of chain orientation from spot to spot along the surface.

In progress, to be reported later, are experiments in which the relative orientation of the mica sheets is varied systematically rather than keeping the optical axes aligned as was done in the data described here.

Spatial heterogeneity is starting to emerge as possibly a general observation for films confined between mica sheets in the surface

(31) Ruths, M.; Granick, S. *Langmuir* **2000**, *16*, 8368−8376.

(32) Liem, H. M.; Etchegoin, P.; Whitehead, K. S.; Bradley, D. D. C. *Adv. Funct. Mater.* **2003**, *13*, 66−72.

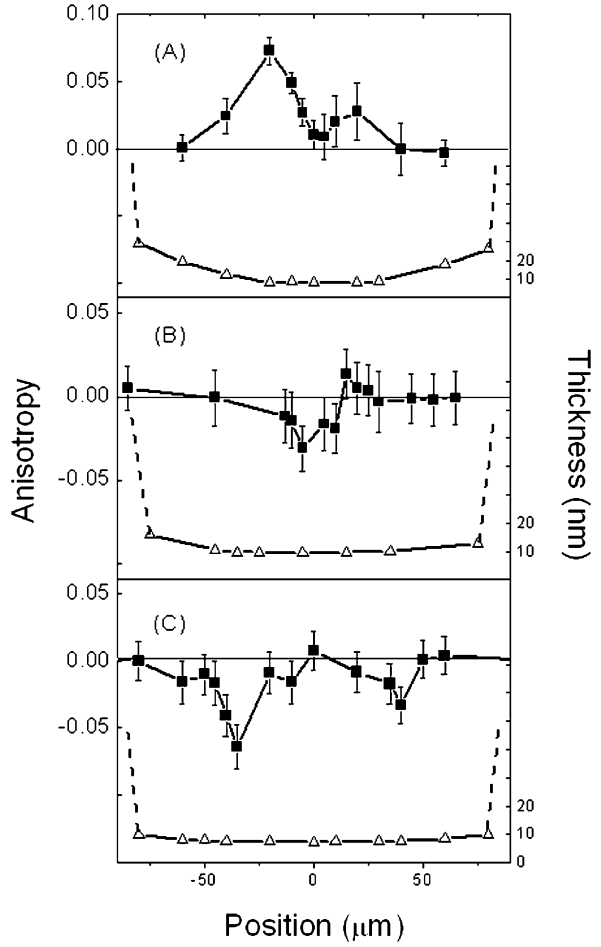

Figure 5. Comparison of local anisotropy and local film thickness for thin films of PDMS melt confined between opposed mica sheets with crystal planes oriented parallel to one another. Squares: local anisotropy of the symmetric methyl stretch in the $x-y$ plane, defined by eq 2, plotted against local spatial position. Triangles: local film thickness, determined by multiple beam interferometry, plotted against local spatial position. Dashed vertical lines indicate the edge of the Hertzian contact. Panels A, B, and C refer to three independent experiments.

forces apparatus. Originally observed in this laboratory to concern translational diffusion,[13,14] it has been confirmed to concern the orientation of embedded fluorescent dyes.[33] While it may be tempting to think that the act of squeezing chains into thin films itself generated preferential ordering but without a preferred direction, it seems unreasonable to think this way when considering that equilibration should be rapid, much more rapid than the many hours involved in each experiment, for chains of the low molecular weights studied. No quantitative explanation is offered at this time.

Vibrational Line Shape Broadens when Chains Are Confined. Studies of small-molecule liquids immersed in porous glasses of radius R find vibrational line shapes to broaden when R decreases, often (depending on the molecule in question) in proportion to $1/R$.[16] Although analysis of vibrational line shape is in general a delicate matter, analysis shows that, when the liquid has a simple shape and the isotropic Raman scattering possesses a symmetric Lorentzian line shape, the mechanism of dephasing can be a simple process such as coupling to low-frequency torsional modes, and the vibrational dephasing time can be calculated by the equation

$$\tau_{\mathrm{vib}} = \frac{1}{\pi c \delta_{\mathrm{iso}}} \tag{2}$$

where δ_{iso} is the bandwidth, the full width at half-maximum of the isotropic Raman band, and c is speed of light. Although methyl groups attached to long PDMS chains are decidedly more complex, applying eq 2 for the sake of argument as a qualitative guide to the data to be presented below would imply that $\tau_{\mathrm{vib}} \approx 0.48$ ps (bulk PDMS melt) and $\tau_{\mathrm{vib}} \approx 0.43$ ps (thinnest confined films). Inspired by the analogy, we have explored how confinement influences vibrational line shape and now proceed to describe the nature of the raw data.

To measure these data most reliably, it was necessary to minimize instrumental broadening. The entrance slit to the spectrometer was narrowed to either 50 or 100 μm, depending on the experiment, which introduces ~3% or ~10% instrumental broadening, respectively, and the bandwidth was corrected for this effect by the following equation

$$\delta_{\mathrm{t}} = \delta_{\mathrm{a}}\left[1 - \left(\frac{S}{\delta_{\mathrm{a}}}\right)^2\right] \tag{3}$$

where δ_{t}, δ_{a}, and S are the true bandwidth, apparent bandwidth, and spectral slit width, respectively. The signals were averaged for at least 1 h.

To obtain the line shape, first the isotropic Raman band is obtained by subtracting the depolarized part from the polarized Raman signal by the equation

$$I_{\mathrm{iso}}(\nu) = I_{\mathrm{pol}}(\nu) - \frac{4}{3} I_{\mathrm{dep}}(\nu) \tag{4}$$

where $I_{\mathrm{iso}}(\nu)$, $I_{\mathrm{pol}}(\nu)$, and $I_{\mathrm{dep}}(\nu)$ are intensities for isotropic, polarized, and depolarized bands, respectively. That the resulting band be symmetric is one requirement for eq 2 to apply. Figure 6A demonstrates that this subtraction leads, when dealing with bulk PDMS, to a symmetric I_{iso} band. However, although this subtraction of I_{dep} was necessary when dealing with thick films, for the thinnest films, the I_{dep} is smaller than the noise level, as illustrated in Figure 6B, although the anisotropy can be determined from the polarized bands. In those cases, the bandwidth of polarized Raman band was considered to be identical to that of the isotropic Raman band.

The fitting in Figure 6A,B showed excellent fit to the Lorentzian function. To the extent that inhomogeneous broadening also contributes, one would expect such data to be better fit by a linear combination of Lorentzian and Gaussian shapes, but this did not improve the quality of fit, so we conclude that the vibrational dephasing was homogeneous.

Figures 7 and 8 show that the dependence of δ_{iso} on system parameters was similar to that of the anisotropy. Specifically, for thin PDMS films on a single mica crystal, the area-averaged δ_{iso} was an apparent linear function of $1/d$. Also, the value of δ_{iso} fluctuated from spot to confocal spot, as illustrated in Figure 8 for a highly confined PDMS film.

These striking trends were not further pursued, because from the available information, it does not seem possible to determine the mechanism of this homogeneous broadening, even though phenomenologically the trends with film thickness are so systematic. In principle, they could simply indicate that the density near the surface is higher than that in the bulk, or they might reflect some kind of elastic coupling, perhaps to phonons or to overtones of other vibrations. They might also reflect anharmonic coupling to higher vibrational energy states. In the future, studies

(33) Alig, A. R. G.; Gourdon, D.; Israelachvili, J. *J. Phys. Chem. B* **2007**, *111*, 95−106.

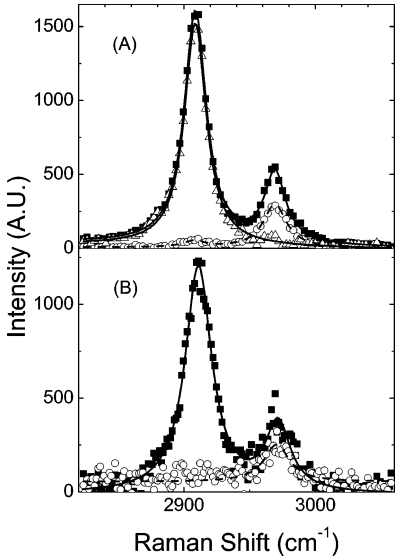

Figure 6. Determination of the isotropic bands of Raman scattering, needed to quantify the vibrational line shape. The isotropic band is determined by subtracting the polarized band from the depolarized band following eq 6. Panel A: bulk PDMS. Panel B: For a film of PDMS 5 nm thick, the polarized band is below the noise level for the data acquisition time of 30 min, although with long data acquisition time the anisotropy can be determined from the polarized bands.

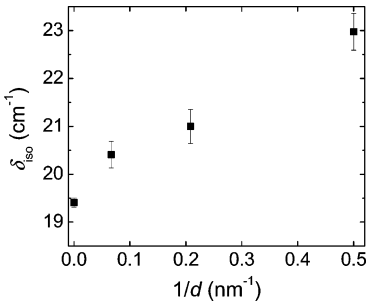

Figure 7. The full width at half-maximum of the isotropic Raman peak centered at 2907 cm^{-1}, δ_{iso}, plotted against inverse film thickness for PDMS melts adsorbed at a single mica surface.

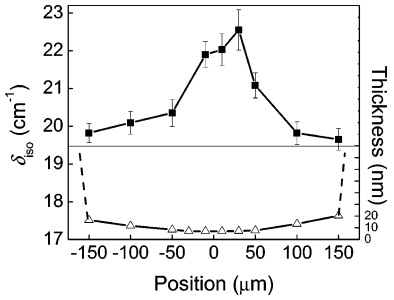

Figure 8. Comparison of local δ_{iso} and local film thickness for thin films of PDMS melt confined between opposed mica sheets with crystal planes oriented parallel to one another. Squares: local δ_{iso} of the symmetric methyl stretch in the $x-y$ plane plotted against local spatial position. Triangles: local film thickness, determined by multiple beam interferometry, plotted against local spatial position. The horizontal line indicates the bandwidth measured for bulk PDMS. Dashed vertical lines indicate the edge of the Hertzian contact.

of temperature dependence may be helpful to give the activation energy of the possible surface perturbation of low-frequency torsional modes.

Outlook

This study shows that the thin-film polymer melt structure is not random in the $x-y$ plane as would be anticipated from classical theory. Anisotropy of the mica unit cell (length scale ~0.5 nm) somehow produces long-range order over the ~300 nm length scale of the confocal spot. Unlike center-of-mass diffusion, which appears to vary systematically according to the Hertzian pressure distribution within a contact spot,[13,14] the structural ordering revealed by these confocal Raman experiments shows no systematic dependence on this quantity.

While there is precedent to observe macroscopic ordering on mica crystals, it is along the direction of the mica crystal axes, and in this respect differs from the apparently randomly selected orientation directions reported here. This may have relevance to the problem of adsorption−desorption kinetics[34−37] as well as polymer diffusion.[38] Seeking precedence for long-range solid-imprinted surface structure possibly analogous to that reported here, we note that, on a single mica surface, materials chemistry can be used to create oriented nanowires that are visible under an optical microscope.[39,40] Also, simulation[41] and experiment[42] show that molecules as small as water form ordered structures on the mica surface. Recently, interesting polymer single-crystal structures were grown on single mica surfaces.[43] When two mica surfaces are slid past one another with liquid crystal[44] or water films[45] in between, the friction is anisotropic, depending on the relative angle between the opposed mica surfaces. The present system—a flexible polymer chain composed of nonpolar repeat units—is decidedly different, however, and we are not aware of any prediction of the strikingly long-range directional interactions reported here.

Although the angle of orientational anisotropy cannot be quantified on the basis of the data we have obtained to date (polarization-dependent measurements over a wider range of azimuthal angles will be needed to accomplish this), these findings may have implications not only for understanding the structure of polymer melts at surfaces, but also for understanding Hertzian contacts in adhesion and tribology. In studies of both adhesion and tribology, it is customary to suppose that confined fluids are the same everywhere except for the local normal pressure. The additional heterogeneity documented here, on length scales of up to ~300 nm, may have implications for understanding the normal and shear mechanical deformation of confined polymer melts.

Acknowledgment. We are indebted to Minsu Kim, a lab mate, and to Mischa Bonn for a helpful conversation. This study was supported by the National Science Foundation under Grant NSF−CMS-0555820. S.C.B. acknowledges partial support from Grant NSF-DMR-06-05947.

LA702295Y

(34) Johnson, H. E.; Douglas, J. F.; Granick, S. *Phys. Rev. Lett.* **1993**, 70, 3267.
(35) Frantz, P.; Granick, S. *Macromolecules* **1994**, 27, 2553.
(36) Schneider, H. M.; Frantz, P.; Granick, S. *Langmuir* **1996**, *12*, 994.
(37) Schneider, H. M.; Granick, S. *Macromolecules* **1992**, *25*, 5054.
(38) Sukhishvili, S. A.; Chen, Y.; Muller, J. D.; Gratton, E.; Schweizer, K. S.; Granick, S. *Macromolecules* **2002**, *35*, 1776.
(39) Akutagawa, T.; Ohta, T.; Hasegawa, T.; Nakamura, T.; Christensen, C. A.; Becher, J. *Proc. Natl. Acad. Sci. U.S.A.* **2002**, *99*, 5028−5033.
(40) Wang, Z. X.; Kong, T.; Zhang, K.; Hu, H. L.; Wang, X. P.; Hou, J. G.; Chen, J. *Mater. Lett.* **2007**, *61*, 251−255.
(41) Wang, J. W.; Kalinichev, A. G.; Kirkpatrick, R. J.; Cygan, R. T. *J. Phys. Chem. B* **2005**, *109*, 15893−15905.
(42) Miranda, P. B.; Xu, L.; Shen, Y. R.; Salmeron, M. *Phys. Rev. Lett.* **1998**, *81*, 5876−5879.
(43) Liu, X. G.; Zhang, Y.; Goswami, D. K.; Okasinski, J. S.; Salaita, K.; Sun, P.; Bedzyk, M. J.; Mirkin, C. A. *Science* **2005**, *307*, 1763−1766.
(44) Ruths, M.; Granick, S. *Langmuir* **2000**, 16, 8368.
(45) Zhu, Y. X.; Granick, S. *Phys. Rev. Lett.* **2001**, *87*, 096104.